Atmos. Chem. Phys. Discuss., 13, 827–862, 2013
www.atmos-chem-phys-discuss.net/13/827/2013/
doi:10.5194/acpd-13-827-2013

Atmospheric Chemistry and Physics Discussions

Sources, trends and regional impacts of fine particulate matter in southern Mississippi Valley: significance of emissions from sources in the Gulf of Mexico coast

M.-C. Chalbot, B. McElroy, and I. G. Kavouras

University of Arkansas for Medical Sciences, Little Rock, Arkansas, USA

Received: 19 October 2012 – Accepted: 22 December 2012 – Published: 9 January 2013

Correspondence to: I. G. Kavouras (ikavouras@uams.edu)

Published by Copernicus Publications on behalf of the European Geosciences Union.

Abstract

The sources of fine particles over a 10 yr period at Little Rock, Arkansas, an urban area in southern Mississippi Valley, were identified by positive matrix factorization. The annual trends of $PM_{2.5}$ and its sources and their associations with the pathways of air mass backward trajectories were examined. Seven sources were apportioned, namely, primary traffic particles, secondary nitrate and sulphate, biomass burning, diesel particles, aged/contaminated sea salt and mineral/road dust, accounting for more than 90 % of measured $PM_{2.5}$ mass. The declining trend of $PM_{2.5}$ mass ($0.4\,\mu g\,m^{-3}\,yr^{-1}$) was related to lower levels of SO_4^{2-} ($0.2\,\mu g\,m^{-3}\,yr^{-1}$) due to SO_2 reductions from point and mobile sources. The slower decline for NO_3^- particles ($0.1\,\mu g\,m^{-3}\,yr^{-1}$) was attributed to the spatial variability of NH_3 in Midwest. The annual variation of biomass burning particles was associated with wildland fires in southeast and northwest US that are sensitive to climate changes. The four regions within 500 km from the receptor site, the Gulf Coast and southeast US accounted cumulatively for more than 65 % of $PM_{2.5}$ mass, nitrate, sulphate and biomass burning aerosol. Overall, more than 50 % of $PM_{2.5}$ and its sources originated from sources outside the state. Sources within the Gulf Coast and western Gulf of Mexico include 65 % of the busiest ports in the US, intense marine traffic within 400 km of the coast burning rich in S diesel, and a large number of offshore oil and natural gas platforms and many refineries along the coast. This approach allowed for quantitatively assessing the impacts of transport from regions representing diverse mixtures of sources and weather conditions for different types of particles. The findings of this effort demonstrated the influences of emission controls on SO_2 and NO_x on $PM_{2.5}$ mass, the potential effect of events (i.e. fires) sensitive to climate change phenomena on air pollution and the potential of offshore activities and shipping emissions to influence air quality in urban areas located more than 1000 km away from the sources.

ACPD
13, 827–862, 2013

1 Introduction

Atmospheric aerosol modifies Earth's energy balance by scattering sunlight back to space, absorbing solar and infrared radiation and changing the microphysical and thermodynamic properties of clouds (Ostrom and Koone, 2000; Lohmann and Feichter, 2001; Quinn and Bates, 2005). Overall, atmospheric aerosols have a negative radiative forcing from $-0.2 \pm 0.2\,\mathrm{W\,m^{-2}}$ to $-0.8 \pm 0.2\,\mathrm{W\,m^{-2}}$, both directly and indirectly, through the cloud albedo effect (IPCC, 2007). Exposures to particulate matter are also associated with acute and chronic health problems and lead to increased mortality rates from respiratory, cardiac and circulatory diseases, increased emergency care visits and hospital admissions for bronchitis and asthma (Brunekreef and Holgate, 2002; Peng et al., 2005; Brunekreef and Forsberg, 2005). In the US, $PM_{2.5}$ (particles with aerodynamic diameter less than 2.5 µm) mass concentrations decreased from 24 % to 28 % between 2001 and 2010 (US EPA, 2012a). These trends were attributed to the significant reductions of gaseous sulfur and nitrogen oxides from coal-fired power plants and mobile sources. These gaseous pollutants are precursors of particulate sulfate and nitrate aerosol, the dominant species of $PM_{2.5}$ aerosol in the Midwest and eastern US. The slower decline on particle mass levels for "cool" months (October to April) as compared to "warm" months was explained by the elevated emissions from residential wood burning and the formation of temperature inversion layers that trigger the accumulation of particles near the ground.

Shipping emissions are recognized as an important source of particulate matter and its precursors around the world (Wang et al., 2003; Deniz et al., 2008; Minguillon et al., 2008). The diesel engines in ships operate on fuel that can have extremely high sulfur content and porphyrin-content rich in V and Ni (termed as bunker oil) and they are subjected to modest emission controls, if any. It is predicted that in the absence of emission controls, SO_2 emissions to the total emissions in the US would increase from 21 % today to 81 %, NO_x emissions would increase to 28 % of total mobile NO_x emissions in the US and $PM_{2.5}$ emissions would almost triple to $170\,000\,\mathrm{t\,yr^{-1}}$ by 2030

ACPD
13, 827–862, 2013

(Corbett et al., 2003; Dalsoren et al., 2009; Eyring et al., 2010). Diesel particles from ships and secondary aerosol from the oxidation of NO_2 and SO_2 are shown to be related to 50 to 500 cancer cases, 750 asthma attacks and 29 pre-mature per million people within 15 miles of the port and influence the air quality in receptor sites far away from the coast (Corbett et al., 2007; Linder et al., 2008).

The Little Rock/North Little Rock Metropolitan Statistical Area (MSA) is a region on the western edge of the southern Mississippi Valley with population of approximately 700 000. 24 h $PM_{2.5}$ levels vary from 1 to 54 $\mu g\,m^{-3}$ over the past 10 yr, with annual $PM_{2.5}$ from 11.4 to 12.6 $\mu g\,m^{-3}$ in 2010. According to 2008 Environmental Protection Agency National Emission Inventory, the highest contributing source to air pollution in prescribed fires contributing 1076 $t\,yr^{-1}$ followed by road dust (617 $tons\,yr^{-1}$). Industrial and mobile sources emit 100 and 300 $tons\,yr^{-1}$ (US EPA, 2012b). Winds are typically from northwest and south/southeast from the Gulf of Mexico enabling transport of particles and its precursors from several regions with diverse and unique characteristics. The objectives were: (i) to apportion the contributions of sources to fine particulate matter in central Arkansas using positive matrix factorization; (ii) to assess the annual trends of $PM_{2.5}$ and its sources; and (iii) to identify and quantify the impacts of regions to fine particle mass and its sources using the trajectory residence time regression analysis. The trajectories residence time regression analysis was previously applied to assess the influences of source regions to sulfate concentrations in continental background sites (Gerbhart et al., 2001; 2006; Xu et al., 2006) and black carbon in Arctic (Huang et al., 2010). Here, we applied this approach on physico-chemically active mixtures of fine particles from different types of sources (local and regional) in an urban area.

ACPD
13, 827–862, 2013

2 Methods

2.1 Sampling site and measurements

The concentrations of $PM_{2.5}$ mass and chemical species measured at the NCore site in North Little Rock (EPA AIRS ID: 051190007 Lat.: 34.756072; Long.: −92.281139) for the 2002–2010 period are retrieved from US Environmental Protection Agency's Air Quality System (AQS). The NCore network (previously known as $PM_{2.5}$ Chemical Speciaton Network) is comprised of 63 urban sites and 18 rural sites across the US. In each site, 1 h and 24 h $PM_{2.5}$ mass, 24 h $PM_{10-2.5}$ mass, $PM_{2.5}$ chemical speciation, NO_x, NO_y, O_3, SO_2, CO were measured. Filter sampling was done in 1 every 3 days frequency using a four channel speciation sampler (Demokritou et al., 2001). Elements (from Na to U) were measured by spectroscopy (X-ray fluorescence, PIXE, ICP, ICP-MS), water-soluble ions (sulfate, nitrate, chloride, ammonium, sodium, potassium, calcium and magnesium) by ion chromatography, atomic absorption, colorimetry and elemental, four fractions of organic carbon organic (evolved from ambient to 140 °C for OC1 (volatile), from 140 °C to 280 °C for OC2 (semivolatile), from 280 °C to 480 °C for OC3 (nonvolatile) and from 480 °C to 580 °C for OC4 (nonvolatile)) and carbonate carbon by thermal optical reflectance (TOR) method.

In Little Rock, the NCore site is located in a park adjacent to the intersection of Pike Av and River Rd in North Little Rock, AR by the Arkansas River. The annual average daily traffic (AADT) on these two roads in very limited (no estimates are provided by Arkansas State Highway and Transportation Department). The streets with the highest AADT are W. Riverfront Dr and W. Broadway St (500 km northwest of the site) with less than 10 000 vehicles/day, respectively (ASHTD, 2011). The site is classified as commercial/neighborhood by EPA.

ACPD
13, 827–862, 2013

2.2 Positive matrix factorization

In PMF, the concentrations of m-aerosol species for n-sampling days are described by sum of the product of the source contribution (G(nxp)) and the source profile matrix (F(pxm)) where p is the number of sources and, the residual component (E(nxm)) (Paatero and Tapper, 1994; Paatero, 1997) (Eq. 1) through a solution that minimizes the objective function (Q in Eq. 2) based on measurements uncertainties:

$$X(\text{nxm}) = G(\text{nxp}) \times F(\text{pxm}) + E(\text{nxm}) \tag{1}$$

$$Q = \sum_{i}^{n} \sum_{k=1}^{m} \left[\frac{x_{ik} - \sum_{k=1}^{m} (g_{ik} \times f_{kj})}{\sigma_{ij}} \right] \tag{2}$$

where x_{ij} and σ_{ij} are the concentration and associated uncertainty of j-species in i-sample, g_{ik} is the contribution of the k-factor to particle mass in i-sample and f_{kj} is the mass fraction of j-species on k-factor. The PMF2 algorithm applies a least-squares approach by considering that sources profiles and contributions are not negative during the optimization analysis. The F_{peak} values controls the subtraction of the profiles from each factor to eliminate the remaining rotational ambiguity. The optimum number of factors (sources) and the rotation (controlled by the F_{peak} value) lies with the mathematical solution in which Q remains relatively constant, the highest individual column mean (IM) and standard deviation (IS) from the scaled residual matrix drop significantly and the highest element in rotmat increases (Paatero et al., 2002; 2005):

$$\text{IM} = \max_{j=1\ldots m} \left(\frac{1}{n} \sum_{i=1}^{n} r_{ij} \right) \tag{3}$$

$$\text{IS} = \max_{j=1\ldots m} \left(\frac{1}{n-1} \sum_{i=1}^{n} (r_{ij} - r_j)^2 \right) \tag{4}$$

ACPD
13, 827–862, 2013

where r_{ij} and r_j are the individual and mean residuals, respectively. The rotmat matrix evaluates the rotational freedom of the solution, with the maximum value of the matrix being indicative of the case with the largest rotational freedom. Missing concentration data are replaced by the geometric mean of the measured concentrations while missing uncertainties are substituted by four times the geometric mean of measured uncertainties. In this effort, we run the PMF2 model in the robust method with an $\alpha = 4.0$ using the error model "–12" (that uses observed values). The α value defines the distance of outliers ($\alpha\sigma_{ij}$) from the fitted value in order to include them into the analysis. The error model determined the s_{ij} values as follows:

$$s_{ij} = t_{ij} + v_{ij}|x_{ij}| \quad (5)$$

where t_{ij} and v_{ij} are the uncertainties and relative errors of x_{ij}. In our case, a seven factor model with a rotation with $F_{peak} = +0.2$ was selected. It is selected on trial and error analysis of the solutions and by comparison of the source profiles with previous studies. The agreement between the calculated and estimated mass concentrations was examined by the percent root mean square error (%RMSE).

2.3 Residence time regression analysis

Five (5) day back trajectories were generated every 1 h using the NOAA Hybrid Single Particle Langangian Trajectory (HYSPLIT) model (Draxler, 2007) with the hemispheric Global Data Assimilation System (GDAS) meteorological data as inputs beginning at 00:00 UTC (a total of 2880 trajectory points (24 trajectories per day × 5 days backward per trajectory × 24 h per trajectory day) per day). The trajectory starting height was defined at 500 m based on climatological mean boundary layer heights in the United States showing that a 500 m starting height would usually be in the boundary layer (Seidel et al., 2012). Trajectories calculated at lower altitude are subject to interference from topography, while trajectories at higher altitude would have been above the mixed layer at times and not representative of the air mass in the mixed layer (Kavouras et al., 2013). The residence time for each 0.5° × 0.5° cells was equal to the sum of

ACPD
13, 827–862, 2013

the number of trajectories points (Ashbaugh et al., 1985; Poirot and Wishinski, 1986). The geographical domain for the trajectory regression analysis covered all cells with estimated residence time at least 72 h over the entire monitoring period (∼ 1 ‰).

The source regions included four regions (5° × 5°) around the monitoring site to describe local/state contributions and 16 source regions considering that the geographic size of the source regions should increase with distance from the urban area of each source region (Fig. 1). The four local source regions were:

- Northwest (northwest Arkansas, eastern Oklahoma and southeast Missouri),
- Northeast (northeast Arkansas, western Tennessee including Memphis and northeast Mississippi),
- Southeast (southeast Arkansas, eastern Louisiana including Baton Rouge and New Orleans) and,
- Southwest (southwest Arkansas and northwest Texas).

The remaining sixteen source regions included:

- Three regions in Canada (west, central and east),
- Pacific Northwest (Washington, Oregon, Idaho, Montana, northern California, northern Nevada, northern Utah and northwest Colorado),
- California and Pacific (Southern California and southern Nevada),
- Southwest US (Arizona, southern Utah, western New Mexico and northeast Mexico),
- North Plains (North Dakota, South Dakota, Nebraska and northeast Colorado),
- Central Texas (eastern New Mexico and central Texas including all the urban areas except Houston, Oklahoma and Kansas),

ACPD
13, 827–862, 2013

- Southertn Texas and northeast Mexico,
- Upper Midwest (Minnesota, Wisconsin, Illinois and northern Missouri),
- Gulf Coast (eastern Texas including Houston, southern Louisiana), Great Lakes (Indiana, Ohio and Michigan),
- Southeast US (Kentucky, Tenneessee, Alabama, Georgia, South Carolina, western Virginia and western North Carolina),
- Florida and Cuba, Eastern US (New England, Pennsylvania, eastern Virginia and eastern North Carolina) and,
- Caribbean Sea.

Because of the definition of the local regions, the impact of sources within the Little Rock/North Little Rock metropolitan area cannot be separated from the sources within the state. The definition of a region encompassing (e.g. 100 × 100 km centered at the site) would only add a significant amount of ambiquity into the model because every single trajectory ends at the site, thus the residence time would be the same.

The time that an air mass spent over these source regions was computed by summing the residence times of cells that fell within each region. The relationship between particle mass concentrations (y_i, in $\mu g\,m^{-3}$) and the time that air spends over each region (t_j, in h) is determined using the Tracer Mass Balance (TrMB) model (Eq. 6) (Pitchford and Pitchford, 1985; Green et al., 2003; Xu et al., 2006):

$$y_i = \sum_{j=1}^{20} C_j + a = \sum_{j=1}^{20} t_j \beta_j + \alpha \quad (6)$$

where C_j (in $\mu g\,m^{-3}$) is the contribution of j-source region on i-sample, β_j (in $\mu g\,(m^{-3}\,h^{-1})$) are the impact factors of regions describing the combined outcome of emissions from the area, aging and pollutants removed due to gravitational settling,

ACPD
13, 827–862, 2013

turbulent mix-out, and wet deposition during transport to the receptor site. The intercept, α, accounts for contributions from source regions outside the study domain. We estimated the source contributions by running the TrMB model with and without the intercept. In our study, we included all cells in which the air masses spent at least 72 h over the study period; thus contributions from sources outside the regions described above may be negligible. Xu et al. (2006) showed that the computed contributions using the TrMB approach with and without the intercept are statistically insignificant and they represent the upper and lower estimates of the contributions, respectively.

3 Results and discussion

3.1 Types of fine aerosol

Table 1 shows the values of concentration diagnostic ratios and the types of $PM_{2.5}$ aerosol in Little Rock for the 2002–2010 period. Sulfur (S) was present as sulfate (SO_4^{2-}) with sulfate-to-sulfur ratio of 3.59 ± 0.35. The NH_4^+/SO_4^{2-} molar ratio (2.06 ± 0.04) suggested that sulfate aerosols were in ammonium sulfate ($(NH_4)_2SO_4$) form (Malm et al., 2002). The OC/EC ratios (6.12 ± 2.11) indicated a mixture of primary and secondary organic aerosol from various sources. OC/EC values lower than 1.1 were indicative of primary traffic emissions, while OC/EC values higher than 2.0 have been observed for coal and biomass combustion as well as secondary organic aerosol (Cachier et al., 1989; Chow et al., 1996; Watson et al., 2001; Turpin and Lim, 2001). Soluble potassium (K^+) accounted for 72 % of total K suggesting the significant impact of biomass burning emissions. Salts in soil also contribute about 20 % of K^+. Ratios of Al/Si (0.48 ± 0.03) K/Fe (1.06 ± 0.06) and Al/Ca (1.76 ± 0.07) were comparable to those determined for samples collected at the Interagency Monitoring of Protected Visibility Environments (IMPROVE) sites in the Midwest and eastern United States (Hand et al., 2012).

ACPD
13, 827–862, 2013

The IMPROVE mass reconstruction scheme was applied to reconstruct aerosol mass into four major species, namely secondary inorganic, organic, light-absorbing carbon, and soil (Eqs. 7–10):

$$\text{Reconstructed PM} = [\text{EC}] + [\text{OM}] + [\text{Secondary Inorganic}] + [\text{Soil}] \quad (7)$$

$$\text{where } [\text{OM}] = 1.6 \cdot [\text{OC}] \quad (8)$$

$$[\text{Secondary Inorganic}] = 1.29 \cdot [NO_3^-] + 0.944 \cdot [NH_4^+] + 1.02 \cdot [SO_4^{2-}] \quad (9)$$

$$[\text{Soil}] = 2.2 \cdot [\text{Al}] + 2.49 \cdot [\text{Si}] + 1.63 \cdot [\text{Ca}] + 2.42 \cdot [\text{Fe}] + 1.94 \cdot [\text{Ti}] \quad (10)$$

where [EC], [OC], $[NO_3^-]$, $[NH_4^+]$, $[SO_4^{2-}]$, [Al], [Si], [Ca], [Fe] and [Ti] are the elemental carbon, organic carbon, nitrate, ammonium, sulfate, aluminum, silica, calcium, iron and titanium concentrations (in $\mu g\,m^{-3}$), respectively. Nitrate may also be associated with coarse particles from neutralization of gas phase nitric acid with sea salt or calcium carbonate. We assumed a conversion factor of 1.6 which is typically used for urban $PM_{2.5}$ atmospheric aerosol. Higher conversion factors were suggested for rural $PM_{2.5}$ aerosol (2.1 ± 0.2) and IMPROVE background sites (1.7 ± 0.2) to reflect the presence of oxygenated functional organic compounds formed during transport (Turpin and Lim, 2001; Malm and Hand, 2007). Soil mass concentration [SOIL] was estimated as the sum of the elements present in the soil as oxides. Carbonaceous aerosol (OM and EC) accounted for 56 % of $PM_{2.5}$ mass with OM being the abundant component. Sulfate represented 29 % of $PM_{2.5}$ mass, while nitrate and mineral dust contributed approximately 8 % and 7 %, respectively.

3.2 Sources of fine aerosol

The good agreement between measured $PM_{2.5}$ and predicted (using the seven-factor PMF model) $PM_{2.5}$ mass concentrations (slope of 0.84 ± 0.02, an intercept of $0.8 \pm 0.3\,\mu g\,m^{-3}$ and $R = 0.90$; Fig. 2) was indicative of a physically meaningful solution explaining most of the variability of fine particles mass (%RMSE of 3.3 % for

ACPD
13, 827–862, 2013

$PM_{2.5}$ mass and less than 15 % for individual chemical species). The difference was attributable to secondary organic aerosol formed from the condensation of biogenic (e.g. isoprene and terpenes) hydrocarbons which cannot be resolved using elemental tracers, ionic composition and total EC/OC concentrations (Hu et al., 2010). The profiles of the seven retained factors and their contributions to 24 h $PM_{2.5}$ mass concentrations are shown in Figs. 3 and 4, respectively. The mean contribution of each source on $PM_{2.5}$ mass concentration is presented in Table 2. The seven factors were attributed to specific sources of fine particles based on the loadings of individual chemical species. The profiles were comparable to those computed in other Midwestern areas (Kim et al., 2005; Lee et al., 2006).

The first factor was assigned to primary particulate matter from gasoline and diesel vehicles with high contributions of OC (total and OC_1, OC_2, OC_3 and OC_4), EC, S, SO_4^{2-}, K, K^+ and heavy metals (Zn, Cr, Co) typically found in tailpipe emissions (Lough et al., 2005). Soil elements (Al, Si, Fe, Ca) were also associated, indicating the possible influence of contaminated road dust released into the air by the friction between the tires and pavement as a vehicle travels. Primary traffic emissions were responsible for $0.3 \pm 0.2\,\mu g\,m^{-3}$ of $PM_{2.5}$ mass (Table 2) with no seasonal variation (Fig. 4a). The contributions to $PM_{2.5}$ mass were higher than $4\,\mu g\,m^{-3}$ for a limited number of episodes in early summer of 2005 to 2009.

The second factor was attributed to secondary NO_3^- with high contributions to NO_3^-, NH_4^+, OC and SO_4^{2-}. The minor contributions to EC and heavy metals found in primary particles indicated a mixture of local and regional influences. The contribution of particulate NO_3^- to $PM_{2.5}$ mass was $1.1 \pm 0.3\,\mu g\,m^{-3}$ which was comparable to the reconstructed concentration of nitrate particles using the IMPROVE scheme (Table 1). A clear seasonal profile with the highest contribution being measured in the winter was observed due to lower ambient temperatures promoting the gas-to-particles conversion of HNO_3 (Fig. 4b).

The third factor showed strong contributions to OC, SO_4^{2-}, Ni, V, Fe, Mn and other heavy metals and was assigned to diesel emissions other than vehicles. This factor

ACPD
13, 827–862, 2013

also demonstrated high contributions to OC, EC, S, SO_4^{2-}, NO_3^-, Ni and V indicating the possible infuence of transport. The impact of harbor and shipping emissions on fine particle levels in inland locations is previously observed. In our case, the Gulf Coast in Louisiana and eastern Texas (i.e. Houston) is characterized by increased marine traffic and many industrial operations (i.e. oil refineries). This may include diesel particles from rail engines and coal-fired power plants. It accounted for $1.2 \pm 0.2\,\mu g\,m^{-3}$ of $PM_{2.5}$ mass (Table 2) with no seasonal variability (Fig. 4c). Episodes of high contributions to $PM_{2.5}$ were mostly observed before 2007.

The high concentrations of Na, Na^+ and Cl on the fourth factor suggested the contribution of aerosol with marine origin (i.e. sea salt) possible from the Gulf Coast. While sea salt particles are typically found in the coarse mode, a fraction of them is associated with fine particles (Teinila et al., 2000). This factor also correlated with OC, EC, S, SO_4^2 and NO_3^- indicating contamination during transport. This factor contributed, on average, $1.4 \pm 0.4\,\mu g\,m^{-3}$ on $PM_{2.5}$ mass concentration. Slightly higher contributions were computed in spring than those measured in winter and summer (Fig. 4d).

The fifth factor showed strong contribution to elemental S, SO_4^{2-}, NH_4^+ and to a lesser extent to EC and OC. It was attributed to secondary sulfate, the primary type of fine particles in Midwest. This source accounted for 37.5 % ($4.8 \pm 0.4\,\mu g\,m^{-3}$) of $PM_{2.5}$. A weak seasonal variability was identified in 2002–2005 with contributions of up to $30\,\mu g\,m^{-3}$ on $PM_{2.5}$ mass.

Mineral dust was identified as a source of $PM_{2.5}$ in Little Rock with high contributions to Al, Si, Ca, Fe, and Ti. In addition, fractions of OC, EC and other elements, such as Mg and Mn were also associated with this factor indicating a mixture of road and mineral dust. The contribution of road dust to $PM_{2.5}$ mass was $1.0 \pm 0.1\,\mu g\,m^{-3}$ with the highest contributions being observed in the summer. Prospero (1999) showed that the transatlantic transport of Saharan dust was manifested by synoptic scale systems affecting large areas in southeastern US. The maximum dust concentrations ($8.4–16.3\,\mu g\,m^{-3}$) in southern Florida were observed in summer months (June–August). The examination of individual 8-day trajectories showed transport from Atlantic Ocean, while GOES

ACPD
13, 827–862, 2013

imagery illustrated dust episodes in 2005 and 2008 over Canary Islands. As a results, the seasonal trend of mineral dust in Little Rock suggested the possible influence of long range transport (Fig. 4a, f).

Lastly, biomass burning was identified because of the high contributions to OC, EC and moderate amounts of K, K^+, NO_3^-, S and SO_4^{2-}. This source contributed $3.0 \pm 0.5\,\mu g\,m^{-3}$ to $PM_{2.5}$ mass with very little variability (from 1 to $9\,\mu g\,m^{-3}$) throughout the year. The absence of a seasonal profile was corroborated by residential wood burning in the winter and the impacts of recreational, prescribed and wildland fires in spring, summer and fall.

3.3 Annual trends of fine particles and its sources

Ordinary least squares (OLS) regression analysis of deseasonalized monthly average $PM_{2.5}$ mass and source contributions was used to determine the annual trends without the seasonal component (Jaffe and Ray, 2007). Table 3 presents the annual trends (absolute and relative compared to 2002) of $PM_{2.5}$ mass concentrations and the seven source ($\mu g\,(m^{-3}\,yr^{-1})$). The observed trends were statistically significant for $PM_{2.5}$ mass ($-0.4\,\mu g\,(m^{-3}\,yr^{-1})$; $-2.9\,\%$), secondary nitrate ($0.09\mu g\,(m^{-3}\,yr^{-1})$; $-7\,\%$), secondary sulfate ($0.2\mu g\,(m^{-3}\,yr^{-1})$; $-3.4\,\%$) and diesel particles ($0.11\,\mu g\,(m^{-3}\,yr^{-1})$; $-7.1\,\%$). The mean annual concentrations of NO_3^- and SO_4^{2-} dropped from $1.3\,\mu g\,m^{-3}$ in 2002 to $1.0\,\mu g\,m^{-3}$ in 2010 for NO_3^- and, from $6.0\,\mu g\,m^{-3}$ in 2002 to $3.3\,\mu g\,m^{-3}$ in 2010. The observed decrease for SO_4^{2-} was comparable to the reductions of SO_2 emissions nationally (from 14 774 tons yr^{-1} in 2002 to 7478 tons yr^{-1} in 2010; 49 %) (EPA, 2012b). NO_x emissions were reduced by 30 % (from 21,135 tons yr^{-1} in 2002 to 14 717 tons yr^{-1} ion 2010). Pitchford et al. (2012) attributed the discrepancy between reductions in NO_x emissions and particulate NO_3^- levels to the availability of gaseous NH_3 to react with HNO_3 and form NH_4NO_3 particles and the thermodynamic coupling of the SO_4^{2-} and NO_3^- formation mechanisms. They concluded that reductions of particulate SO_4^{2-} (due

ACPD
13, 827–862, 2013

to reduced SO_2 emissions) would cause an increase to particulate NO_3^-, but the overall $PM_{2.5}$ would be reduced. The significance of this non-linear relationship may be crucial for southern Midwest because of the high NH_3 emissions in southern states.

For mineral dust (−0.8 %), biomass burning (−1.2 %) and aged/contaminated sea salt (+3.9 %), statistically insignificant trends were computed (from −0.02 to +0.03 μg (m^{-3} yr^{-1})), because these sources may be influenced by weather patterns and climatology. Figure 5 illustrates the monthly contributions of biomass burning to $PM_{2.5}$ (and fitting) and the area burnt (in acres) by wildland fires in the US (data obtained from the National Interagency Fire Center) during the 2002–2010 period. While episodic high contributions from biomass burning were also computed for years with reduced burned areas by wildfires (2003 and 2009 in Fig. 5), on average, the trend of biomass contributions was comparable to that of the burned areas by fires in the US. During the 2004–2007, wildfires burned more than 8 million acres per year in the US as compared to less than 5 million acres in 2003 and 2008. This increase was partially attributed to sequencing of El Niño events (wet) and La Niña events (dry) by promoting the growth of fuels and the subsequently dry them out over a period of years (Crimmins and Comrie, 2004; Littell et al., 2009). During the study period, four El Niño and two La Niña events were identified. Weak El-Niño events were observed in 2004 and 2006 and moderate El-Niño events were identified in 2002 and 2009. In these climate events, equatorial Pacific Ocean is warmer than usual, altering the weather conditions around the world. These conditions favored larger and destructive wildfires around the country. On the contrary, the colder Equatorial Pacific in La Niña events facilitates colder than normal conditions in northwest US and warmer than normal in southeast US, reducing the fire risks.

3.4 Regional contributions

Figure 6 shows the spatial variation of residence times in winter, spring, summer and fall. These maps show clear seasonal differences between air masses near the ground. More specifically, winter trajectories originated often from north/northwest over upper

ACPD
13, 827–862, 2013

Midwest, North Plains, and traveled through the Mississipi Valley prior to their arrival in central Arkansas. In spring and fall, trajectories demonstrated more local influences by spending most of their time in surrounding states. On the other hand, air masses in the summer extended from northeast to south/southeast covering a larger geographical area from the central midwest to the Gulf of Mexico and Cuba and were not as influenced by topographic restrictions. Thus, these distinctions indicated that air masses in winter may have substantially different compositional characteristics as compared to air masses for the other seasons and particularly in the summer.

Figure 7 shows the mean (± error) of the contributions of each region on $PM_{2.5}$ mass and source contributions for both models with (lower line) and without (upper line) intercept. The differences of the contributions calculated for the two models were negligible (and statistically insignificant within 1 standard error) for NO_3^-, diesel particles, SO_4^{2-}, mineral dust and biomass burning. Some differences were observed for primary traffic particle and aged/contaminated sea salt; however, in these cases, the overall estimated contributions for specific sectors were negligible ($0.2 \pm 0.4\,\mu g\,m^{-3}$). These similarities suggested the robustness of the trajectories regression analysis to determine the spatial distribution of $PM_{2.5}$ mass and source contributions in an urban area. The four regions around the site (NW, NE, SW and SE in Fig. 1), the Gulf Coast and southeast US contributed 42 % ($5.6 \pm 0.9\,\mu g\,m^{-3}$), 16 % ($2.1 \pm 0.3\,\mu g\,m^{-3}$) and 10 % ($1.4 \pm 0.2\,\mu g\,m^{-3}$) of $PM_{2.5}$ mass, with sources within the southwest sector being responsible for $2.1 \pm 0.3\,\mu g\,m^{-3}$ of $PM_{2.5}$. These sectors include the urban areas of Dallas in Texas, Oklahoma City in Oklahoma, Memphis in Tennessee and Baton Rouge in Louisiana and, point sources emitting emitted cumulatively 731,262 tons of $PM_{2.5}$ in 2008 (48 % of national annual $PM_{2.5}$ emissions from point sources) (EPA, 2012b). Moderate contributions from Upper Midwest ($0.8 \pm 0.2\,\mu g\,m^{-3}$) and central Texas ($0.4 \pm 0.2\,\mu g\,m^{-3}$) were also computed. The same areas were responsible for 60 % of primary traffic particles followed by Pacific Northwest (16 % each).

A slightly modified spatial pattern was observed for secondary nitrate particles with 35 % of that being from the southern sectors (SW and SE), 19 % from Pacific

ACPD
13, 827–862, 2013

Northwest and 11 % from Upper Midwest. Minor contributions (3–6 %) were also computed for central Texas and the NW sector. For the two sectors south of Little Rock, the increased nitrate contribution was due to the interaction of NH_3-rich conditions in southern Arkansas and Louisiana with air mass loaded in NO_x/gaseous HNO_3 from metropolitan areas in Texas to form NH_4NO_3 (Pitchford et al., 2012). Furthermore, emissions of other agents such as soil mineral (Ca, K) and sea salt (Na, Mg) off the Gulf Coast and semi-arid areas in northeastern Texas may also neutralize HNO_3 and form stable salts in the aerosol phase. The significant contributions of Pacific Northwest and North Plains domains on NO_3^- levels in central Arkansas were also attributed to neutralization of HNO_3 as the air masses travel over areas (North Plains, Nebraska, Kansas, Missouri, Minnesota, Iowa) with the highest NH_3 emissions in the US and the induced formation of nitrate particles due to typically lower ambient temperatures measured in northern US as compared to those measured in the southern Mississippi Valley.

About 80 % of secondary sulfates ($3.7 \pm 0.3\,\mu g\,m^{-3}$) ($SO_4^{2-}$) and 62 % ($0.7 \pm 0.2\,\mu g\,m^{-3}$) of diesel particles (other than diesel vehicles) were allocated to the four sectors around the receptor site, the Gulf Coast and southeast US. These areas include a large number of SO_2 point sources including coal-fired power plants, oil refineries, off-shore oil and natural gas platforms and ports. In 2008, these sources accounted for 55 % of annual SO_2 emissions in the US (33 % southeast US, 8 % NW, 5 % southeast, 4 % NW and 4 % SW). Two electrical power plants are located within Arkansas emitting approximately 68 000 tons of $SO_2\,yr^{-1}$ (less than 1 % of all SO_2 in the six regions) (one less than 100 km southwest of Little Rock) (EPA, 2012b). Gulf Coast also appeared to be the primary regional contributor for sea salt (25 %; $0.3 \pm 0.2\,\mu g\,m^{-3}$) and mineral dust (55 %, $0.4 \pm 0.1\,\mu g\,m^{-3}$). The area of Gulf Coast includes thirteen of the twenty busiest ports in the US with Houston and New Orleans being among the top five (US Army of Engineers, 2010). Marine traffic within 400 km from the land in the western Gulf Coast ranks among the top five busiest areas in the world (more than 1/3 of vessel calls in the US mostly (~ 60 %) from tanker and

ACPD
13, 827–862, 2013

container ships) (Ward and Gallagher, 2010). These ships used oil with high sulfur content from 5 to 4500 ppm. The Gulf Coast region also includes approximately 3000 oil and natural gas platforms producing more than half of crude oil and natural gas production in the US. These platforms emit minor quantities of SO_2 (less than 0.1 % of national SO_2 emissions) but up to 1.5 % and 5.3 % of national NO_x and VOCs emissions.

Approximately 45 % ($1.3 \pm 0.2\,\mu g\,m^{-3}$) of biomass burning originated from the eastern (NE and SE) and SW sectors followed by Gulf Coast (9 %, $0.3 \pm 0.1\,\mu g\,m^{-3}$) and southeast US (8 %, $0.2 \pm 0.1\,\mu g\,m^{-3}$). In these regions, most of emissions are from residential woodburning, recreational, agricultural and prescribed burns. Large fires are infrequently observed mostly in years with prolonged drought conditions. The combined contribution of Pacific Northwest, North Plains and Upper Midwest accounted for 20 % of biomass burning emissions ($0.6 \pm 0.2\,\mu g\,m^{-3}$) mostly from large wildfires in Colorado Rockies forests and agricultural fires. Figure 8 shows the cumulative data of thermal anomalies caused by fire incidents as they were detected by Terra and Aqua MODIS satellites during the 2002–2010 period. The size of the aggregating cells is 0.25° per side. These results indicated many temperature anomalies east and south of the receptor site and in southern Alabama and Georgia with weak/moderate thermal signatures which are typical of small-scale prescribed, agricultural and recreational burns. In addition, a smaller number of temperature anomalies associated with higher temperatures were observed in Kansas, Idaho, Oregon and Washington indicating larger, long-lasting and more intense fire events.

The spatial distribution of regional contributions to $PM_{2.5}$ and its sources was comparable to those modeled for the Caney Creek IMPROVE site located in southwest Arkansas. It is found that sulfate from east Texas, southeast US, and upper Midwest; nitrate from central Midwest, and east Texas as well as organic aerosol from Houston and Arkansas were responsible for the oberved reduction of visibility (ENVIRON, 2007).

ACPD
13, 827–862, 2013

4 Conclusions

The sources of fine particles in central Arkansas for the 2002–2010 period were secondary sulfate (36 %), biomass burning (20 %), aged sea salt (10 %), diesel emissions (9 %), secondary nitrate (8 %), mineral dust (6 %), and primary particulate emissions from vehicles (2 %). The remaining unexplained fine particle mass was attributed to secondary organic aerosol. Strong seasonal variabilities were observed for nitrate (high in the winter) and mineral dust (high in early summer) and a weak seasonal profile (high in the summer) for sulfate for the 2002–2005 period. These trends were consistent with those observed in other urban environments and the dependence on meteorology and precursors emissions. The absence of seasonality of biomass burning emissions were due to contributions from residential wood burning in winter and wildland fires for the other seasons.

Fine particle mass concentrations and the contributions of secondary sulfate declined by 0.4 $\mu g\,m^{-3}$ and 0.2 $\mu g\,m^{-3}\,yr^{-1}$, which is consistent with the reductions on SO_2 emission from point and mobile sources. A slower declining trend was also observed for secondary nitrate despite the significant reductions of NO_x emissions. This was explained by the abundance of NH_3 in Midwest that favors the formation of stable forms of ammonium nitrate particles. The annual variability of biomass burning contributions to fine particle mass correlated very well with the burnt area by fires in the US which is directly related to the frequency of El Nino and La Nina events that are modified by climate change. The impact of transport of fine particles in central Arkansas was assessed by regression against the residence time of air mass in pre-defined regions. The four regions around the receptor site accounted for large fractions of fine particle mass, primary traffic emission, secondary sulfate and biomass burning. The contributions of sources in southeast US and western Gulf Coast were also significant accounting for 30 % of secondary sulfate and contaminated sea salt particles.

In this study, we demonstrated that residence time regression analysis may be successfully used to identify the impacts of emissions from specific regions on particle

ACPD
13, 827–862, 2013

mass and source contributions in urban receptor sites. Through this analysis, the effect of events associated with climate change on $PM_{2.5}$ from biomass burning was identified and the role of meteorology and NH_3 emissions was observed. In addition, the impact of shipping activities in western Gulf of Mexico and coastal cities on fine particles was assessed; a region of potential interest as emissions from point (i.e. power plants) and mobile sources are decreasing while marine traffic and associated emissions of gaseous precursors and particles will grow substantially.

Acknowledgements. This study was partially funded by the UAMS Center for Diversity Affairs Arkansas Commitment Scholars.

References

ASHTD (Arkansas State Highway and Transportation Department): Annual Average Daily Traffic Estimates, 2011.

Ashbaugh, L. L., Malm, W. C., and Sadeh, W. Z.: A residence time probability analysis of sulfur concentrations at Grand Canyon National Park, Atmos. Environ., 19, 1263–1270, 1985.

Brunekreef, B. and Forsberg, B.: Epidemiological evidence of effects of coarse airborne particles on health, Eur. Respir. J., 26, 309–318, 2005.

Brunekreef, B. and Holgate, S. T.: Air pollution and health, Lancet, 360, 1233–1242, 2002.

Cachier, H., Bremond, M. P., and Buat-Menard, P.: Carbonaceous aerosols from different tropical biomass burning sources, Nature, 340, 371–373, 1989.

Chow, J. C., Watson, J. G., Lu, Z., Lowenthal, D. H., Frazier, C. A., Solomon, P. A., and Thuillier, R. H.: Descriptive analysis of $PM_{2.5}$ and PM_{10} at regionally representative locations during 25 SJVAQS/AUSPEX, Atmos. Environ., 30, 2079–2112, 1996.

Corbett, J. J. and Koehler, H. W.: Updated emissions from ocean shipping, J. Geophys. Res.-Atmos., 108, 4650–4666, doi:10.1029/2003JD003751, 2003.

Corbett, J. J., Winebrake, J. J., Green, E. H., Kasibhatla, P., Eyring, V., and Lauer, A.: Mortality from ship emissions: a global assessment, Environ. Sci. Technol., 41, 8512–8518, 2007.

Crimmins, M. and Comrie, A.: Wildfire-climate interactions across southeast Arizona, Int. J. Wildland Fire, 13, 455–466, 2004.

ACPD

13, 827–862, 2013

Dalsøren, S. B., Eide, M. S., Endresen, Ø., Mjelde, A., Gravir, G., and Isaksen, I. S. A.: Update on emissions and environmental impacts from the international fleet of ships: the contribution from major ship types and ports, Atmos. Chem. Phys., 9, 2171–2194, doi:10.5194/acp-9-2171-2009, 2009.

Demokritou, P., Kavouras, I. G., Harrison, D., and Koutrakis, P.: Development and evaluation of an impactor for a $PM_{2.5}$ speciation sampler, J. Air Waste Manage., 51, 514–523, 2001.

Deniz, C. and Durmisoglu, Y.: Estimating shipping emissions in the region of the Sea of Marmara, Turkey, Sci. Total Environ., 390, 255–26, 2008.

Draxler, R. R.: Demonstration of a global modeling methodology to determine the relative importance of local and long-distance sources, Atmos. Environ., 41, 776–789, 2007.

ENVIRON (Environ International Corporation and University of California at Riverside): Technical Support Document for CENRAP Emissions and Air Quality Modeling to Support Regional Haze State Implementation Plans, available at: http://www.dnr.mo.gov/ENV/apcp/docs/appendixf-1.pdf, 2007.

Eyring, V., Isaksen, I. S. A., Berntsen, T., Collins, W. J., Corbett, J. J., Endressen, O., Grainger, R. G., Moldanova, J., Schlager, H., and Stevenson, D. S.: Transport impacts on atmosphere and climate: shipping, Atmos. Environ., 44, 4735–4771, 2010.

Gebhart, K. A., Kreidenweis, S., and Malm, W. C.: Back-trajectory analyses of fine particulate matter measured at Big Bend National Park in the historical database and the 1996 scoping study, Sci. Total Environ., 276, 185–204, 2001.

Gebhart, K. A., Schichtel, B. A., Barna, M. G., and Malm, W. C.: Quantitative back-trajectory apportionment of sources of particulate sulfate at Big Bend National Park, TX, Atmos. Environ., 40, 2436–2448, 2006.

Gray, H. A., Cass, G. R., Huntzicker, J. J., Heyerdahl, E. K., and Rau, J. A.: Characteristics of atmospheric organic and elemental carbon particle concentrations in Los Angeles, Environ. Sci. Technol., 20, 580–582, 1986.

Green, M., Kuhns, H., Pitchford, M., Dietz, R., Ashbaugh, L., and Watson, T.: Application of the tracer-aerosol gradient interpretive technique to sulfur attribution for the Big Bend Regional Aerosol and Visibility Observational Study, J. Air Waste Manage., 53, 586–595, 2003.

Hand, J. L., Schichtel, B. A., Pitchford, M., Malm, W. C., and Frank, N. H.: Seasonal composition of remote and urban fine particulate matter in the United States, J. Geophys. Res.-Atmos., 117, D05209, doi:10.1029/2011JD017122, 2012.

ACPD
13, 827–862, 2013

Hu, D., Bian, Q., Lau, A. K. H., and Yu, J. Z.: Source apportioning of primary and secondary organic carbon in summer $PM_{2.5}$ in Hong Kong using positive matrix factorization of secondary and primary organic tracer data, J. Geophys. Res.-Atmos., 115, D16204, doi:10.1029/2009JD012498, 2010.

Huang, L., Gong, S. L., Sharma, S., Lavoué, D., and Jia, C. Q.: A trajectory analysis of atmospheric transport of black carbon aerosols to Canadian high Arctic in winter and spring (1990–2005), Atmos. Chem. Phys., 10, 5065–5073, doi:10.5194/acp-10-5065-2010, 2010.

IPCC (Intergovernmental Panel on Climate Change): Climate Change 2001: The Scientific Basis, edited by: Houghton, J. T., Ding, Y., Griggs, D. J., Noguer, M., van der Linden, P. J., Dai, X., Maskell, K., and Johnson, C. A., Cambridge University press, New York, 2001.

Jaffe, D. and Ray, J.: Increase in surface ozone at rural sites in the western US, Atmos. Environ., 41, 5452–5463, 2007.

Kavouras, I. G., DuBois, D. W., Etyemezian, V., and Nikolich G.: Spatiotemporal variability of ground-level ozone and influence of smoke in Treasure Valley, Idaho, Atmos. Res., doi:10.1016/j.atmosres.2012.12.005, in press, 2013.

Kim, E., Hopke, P. K., Kenski, D. M., and Korber, M.: Sources of fine particles in a rural Midwestern US area, Environ. Sci. Technol., 39, 4953–4960, 2005.

Lee J. H., Hopket P. K., and Turner, J. R.: Source identification of airborne $PM_{2.5}$ at the St. Louis–Midwest supersite, J. Geophys. Res.-Atmos., 111, D10S10, doi:10.1029/2005JD006329, 2006.

Linder, S. H., Marko, D., and Sexton, K.: Cumulative cancer risk from air pollution in Houston: disparities in risk burden and social disadvantage, Environ. Sci. Technol., 42, 4312–4322, 2008.

Littell, J. S., McKenzie, D., Peterson, D. L., and Westerling, A. L.: Climate and wildfire area burned in western U.S. ecoprovinces, 1916–2003, Ecol. Appl., 19, 1003–1021, 2009.

Lohmann, U. and Feichter, J.: Can the direct and semi-direct aerosol effect compete with the indirect effect on a global scale, Geophys. Res. Lett., 28, 159–161, 2001.

Lough, G. C., Schauer, J. J., Park, J. S., Shafer, M. M., Deminter, J. T., and Weinstein J. P.: Emissions of metals associated with motor vehicle roadways, Environ. Sci. Technol., 39, 826–836, 2005.

Malm, W. C. and Hand, J. L.: An examination of the physical and optical properties of aerosols collected in the IMPROVE program, Atmos. Environ., 41, 3407–3427, doi:10.1016/j.atmosenv.2006.12.012, 2007.

ACPD
13, 827–862, 2013

Malm, W. C., Schichtel, B. A., Ames, R. B., and Gebhart K. A.: A 10-yr spatial and temporal trend of sulfate across the United States, J. Geophys. Res., 107, 4627, doi:10.1029/2002JD002107, 2002.

Malm, W. C., Schichtel, B. A., Pitchford, M. L., Ashbaugh. L. L., and Eldred, R. A.: Spatial and monthly trends in speciated fine particle concentration in the United States, J. Geophys. Res., 109, D03306, doi:10.1029/2003JD003739, 2004.

Minguillon, M. C., Arhami, M., Schauer, J. J., and Sioutas, C.: Seasonal and spatial variation of sources of fine and quasi-ultrafine particulate matter in neighborhoods near the Los Angeles-Long Beach harbor, Atmos. Environ., 42, 7317–7328, 2008.

Ostrom, E. and Noone, K. J.: Vertical profiles of aerosol scattering and absorption measured in-situ during the North Atlantic Aerosol Characterization Experiment (ACE-2), Tellus B, 52, 526–545, 2000.

Paatero, P.: Least-squares formulation of robust non-negative factor analysis, Chem. Intell. Lab. Syst., 37, 23–35, 1997.

Paatero, P. and Tapper, U.: Positive matrix factorization: a non-negative factor model with optimal utilization of error estimates of data values, Environmetrics, 111–126, 1994.

Paatero, P, Hopke, P. K., Song, X.-H., and Ramadan, Z.: Understanding and controlling rotation in factor analytic models, Chem. Intell. Lab. Syst., 60, 253–264, 2002.

Paatero, P., Hopke, P. K., Begum, B. A., and Biswas, S. K.: A graphical diagnostic mehod for assessing the rotation in factor analysitcal models of atmospheric pollution, Atmos. Environ., 39, 193–201, 2005.

Peng, R. D., Dominici, F., Pastor-Barriuso, R., Zeger, S. L., and Samet J. M.: Seasonal analyses of air pollution and mortality in 100 US cities, Am. J. Epidemiol., 161, 585–594, 2005.

Pitchford, M. and Pitchford, A.: Analysis of regional visibility in the Southwest using principal component and back trajectory techniques, Atmos. Environ., 19, 1301–1316, 1985.

Pitchford, M. L., Poirot, R. L., Schichtel, B. A., and Malm, W. C.: Characterization of the winter midwestern particualte nitrate bulge, J. Air Waste Manage., 59, 1061–1069, 2012.

Poirot, R. L. and Wishinski, P. R.: Visibility, sulfate and air mass history associated with the summertime aerosol in northern Vermont, Atmos. Environ., 20, 1457–1469, 1986.

Prospero, J. M.: Long-term measurements of the transport of African mineral dust to the southeastern United States: implications for regional air quality, J. Geophys. Res.-Atmos., 104, 15917–15925, 1999.

ACPD
13, 827–862, 2013

Quinn, P. K. and Bates, T. S.: Regional aerosol properties: comparison of boundary layer measurements from ACE 1, ACE 2, Aeorosols99, INDOEX, ACE Asia, TARFOX and NEAQS, J. Geophys. Res., 110, D14202, doi:10.1029/2004JD004755, 2005.

Seidel, D. J., Zhang, Y., Beljaars, A., Golaz, J.-C., Jacobson, A. R., and Medeiros B.: Climatology of the planetary boundary layer over the continental United States and Europe, J. Geophys. Res., 117, D17106, doi:10.1029/2012JD018143, 2012.

Teinila, K., Kerminen V- M., and Hillamo, R.: A study of size-segregated aerosol chemistry in the Antarctic atmosphere, J. Geophys. Res.-Atmos., 105, 3893–3904, doi:10.1029/1999JD901033, 2000.

Turpin, B. J. and Lim H. J.: Species contributions to $PM_{2.5}$ mass concentrations: revisiting common assumptions for estimating organic mass, Aerosol. Sci.Tech., 35, 602–610, 2001.

US ACE (United States Army Corps of Engineers): U.S. Waterway Data – Principal Ports of the United States, Navigation Data Center Spreadsheets, available at: http://www.ndc.iwr.usace.army.mil//data/datappor.htm, last access: October 2012, 2010.

US DOE (United States Department of Energy): Natural Gas Withdrawals and Production, available at: http://www.eia.gov/dnav/pet/pet_crd_crpdn_adc_mbbl_a.htm, last access: October 2012, 2010.

US DOE (United States Department of Energy): Crude Oil Production, available at: http://www.eia.gov/dnav/pet/pet_crd_crpdn_adc_mbbl_a.htm, last access: October 2012, 2011.

US EPA (United States Environmental Protection Agency), Office of Air Quality Planning and Standards: Our Nation's Air. Status and Trends through 2010, EPA-454/R-12–001, 2012a.

US EPA (United States Environmental Protection Agency), Office of Air Quality Planning and Standards: 2008 National Emissions Inventory, Version 2, available at http://www.epa.gov/ttn/chief/net/2008neiv2/2008_neiv2_tsd_draft.pdf, last access: October 2012, 2012b.

Wang, T., Ding, A. J., Blake, D. R., Zahorowski, W., Poon, C. N., and Li, Y. S.: Chemical characterization of the boundary layer outflow of air pollution to Hong Kong during February–April 2001, J. Geophys. Res.-Atmos., 108, 8787, doi:10.1029/2002JD003272, 2003.

Ward, K. R. and Gallagher, B.: Utilizing vessel traffic and historical bathymetric data to prioritize hydrographic surveys, in: U.S. Hydro, edited by: Steve Barnum, National Ocean Service, The Hydrographic Society of America, April 2011, available at: hypack.com/ushydro/2011, 2011.

ACPD
13, 827–862, 2013

Watson, J. G., Chow, J. C., and Houck, J. E.: PM2.5 chemical source profiles for vehicle exhaust, vegetative burning, geological material, and coal burning in Northwestern Colorado during 1995, Chemosphere, 43, 1141–1151, 2001

Xu, J., DuBois, D., Pitchford, M., Green, M., and Etyemezian, V.: Attribution of sulfate aerosols in Federal Class I areas of the western United States based on trajectory regression analysis, Atmos. Environ., 40, 3433–3447, 2006.

ACPD

13, 827–862, 2013

Table 1. Diagnostic ratio of $PM_{2.5}$ chemical species and major aerosol types in Little Rock, Arkansas.

Ratio	Value (Mean ± error)	Aerosol type	Concentration (Mean ± error; $\mu g\,m^{-3}$)
SO_4^{2-}/S	3.59 ± 0.35	Elemental carbon	0.6 ± 0.1
Molar NH_4^+/SO_4^{2-}	2.06 ± 0.04	Organic mass	7.1 ± 0.9
OC/EC	5.88 ± 0.35	Ammonium sulfate	3.9 ± 0.2
K^+/K	0.72 ± 0.06	Ammonium nitrate	1.1 ± 0.1
Al/Si	0.48 ± 0.03	Soil dust	1.0 ± 0.1
K/Fe	1.06 ± 0.06	Reconstructed $PM_{2.5}$ mass	13.7 ± 1.1
Al/Ca	1.76 ± 0.07	Measured $PM_{2.5}$ mass	13.7 ± 0.8

ACPD
13, 827–862, 2013

Table 2. Source contributions to $PM_{2.5}$ in Little Rock, Arkansas.

Source	Contribution (Mean ± error; $\mu g\,m^{-3}$)
Primary traffic emissions	0.3 ± 0.2
Secondary nitrate	1.1 ± 0.3
Diesel emissions	1.2 ± 0.2
Aged sea salt	1.4 ± 0.4
Secondary sulfate	4.8 ± 0.4
Mineral dust	1.0 ± 0.1
Biomass burning	3.0 ± 0.5
Predicted $PM_{2.5}$ mass	12.8 ± 0.9
Measured $PM_{2.5}$ mass	13.7 ± 0.8

ACPD
13, 827–862, 2013

Table 3. Absolute and relative (to 2002) annual trends for $PM_{2.5}$ and source contributions in Little Rock, Arkansas.

Component/source	Trend ($\mu g\,m^{-3}\,yr^{-1}$)	% Trend per year	*p*-value
$PM_{2.5}$ mass	−0.4	−2.9 %	0.000
Primary traffic emissions	−0.01	−3.4 %	0.254
Secondary nitrate	−0.09	−7.0 %	0.000
Diesel emissions	−0.11	−7.1 %	0.001
Aged sea salt	0.03	3.9 %	0.123
Secondary sulfate	−0.20	−3.4 %	0.001
Mineral dust	−0.01	−0.8 %	0.610
Biomass burning	−0.02	−1.2 %	0.529

ACPD
13, 827–862, 2013

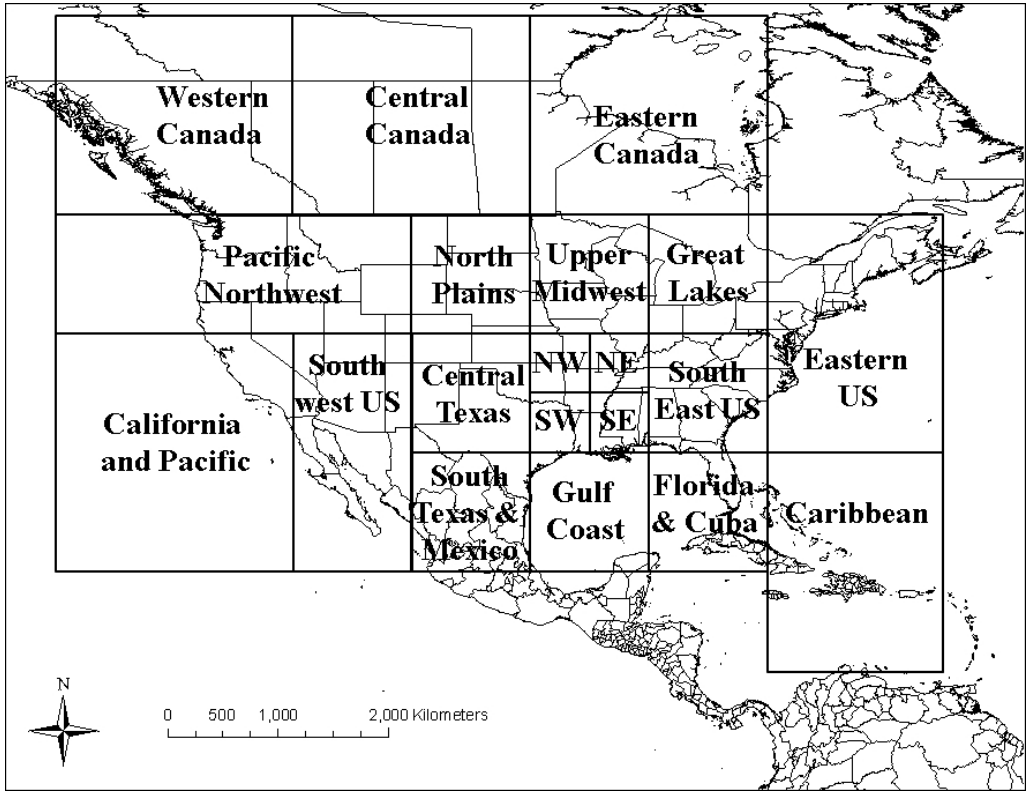

Fig. 1. The predefined source regions for Little Rock, Arkansas.

ACPD
13, 827–862, 2013

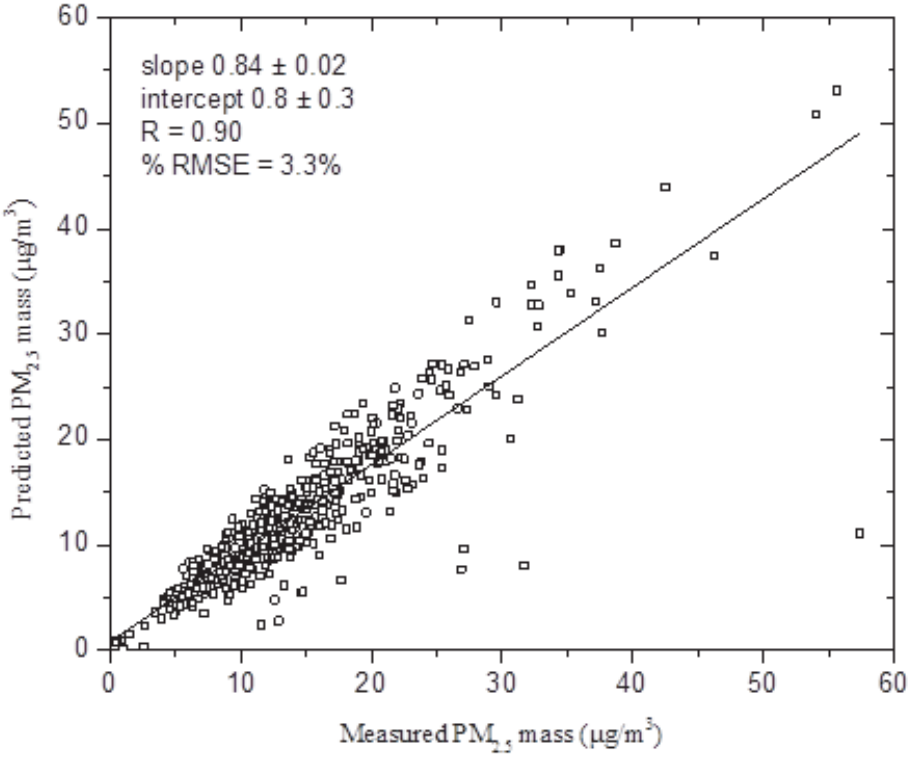

Fig. 2. Comparison of measured and predicted mass concentrations of $PM_{2.5}$ in Little Rock, Arkansas.

ACPD
13, 827–862, 2013

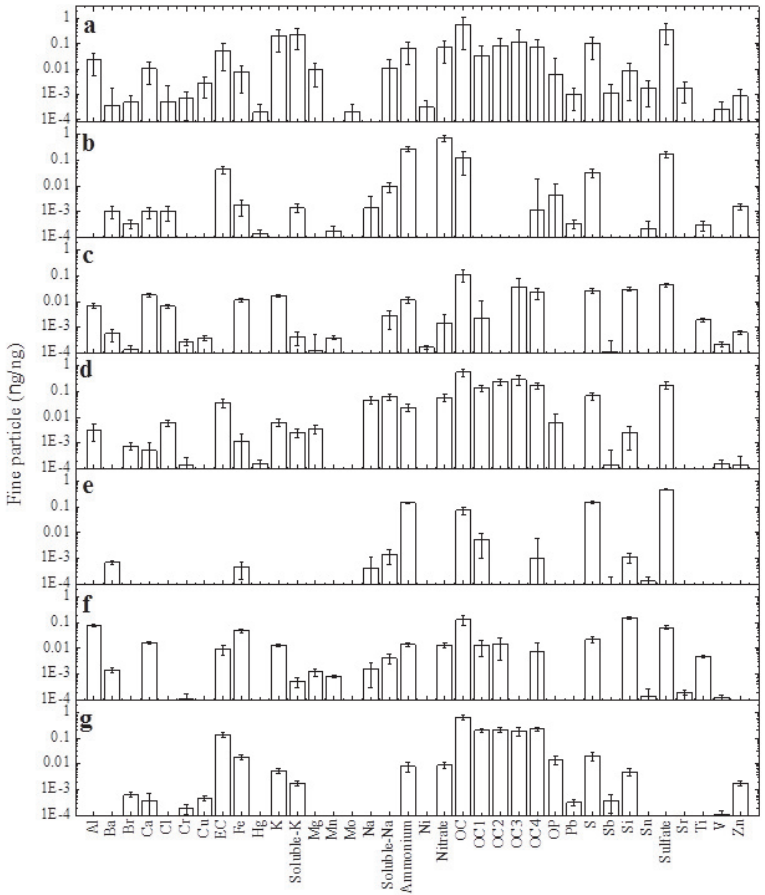

Fig. 3. Profiles of primary traffic particles **(a)**, secondary nitrate **(b)**, diesel emissions **(c)**, aged sea salt **(d)**, secondary sulphate **(e)**, mineral dust **(f)** and biomass burning **(g)** in Little Rock, Arkansas.

ACPD
13, 827–862, 2013

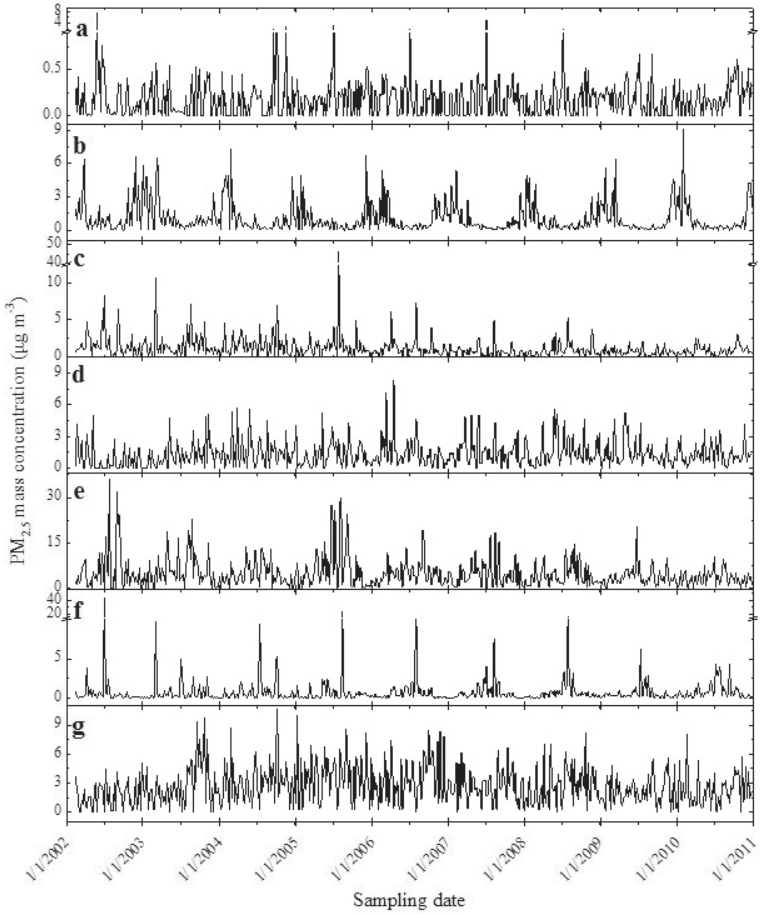

Fig. 4. Contributions of primary traffic particles **(a)**, secondary nitrate **(b)**, diesel emissions **(c)**, aged sea salt **(d)**, secondary sulphate **(e)**, mineral dust **(f)** and biomass burning **(g)** on $PM_{2.5}$ mass in Little Rock, Arkansas.

ACPD
13, 827–862, 2013

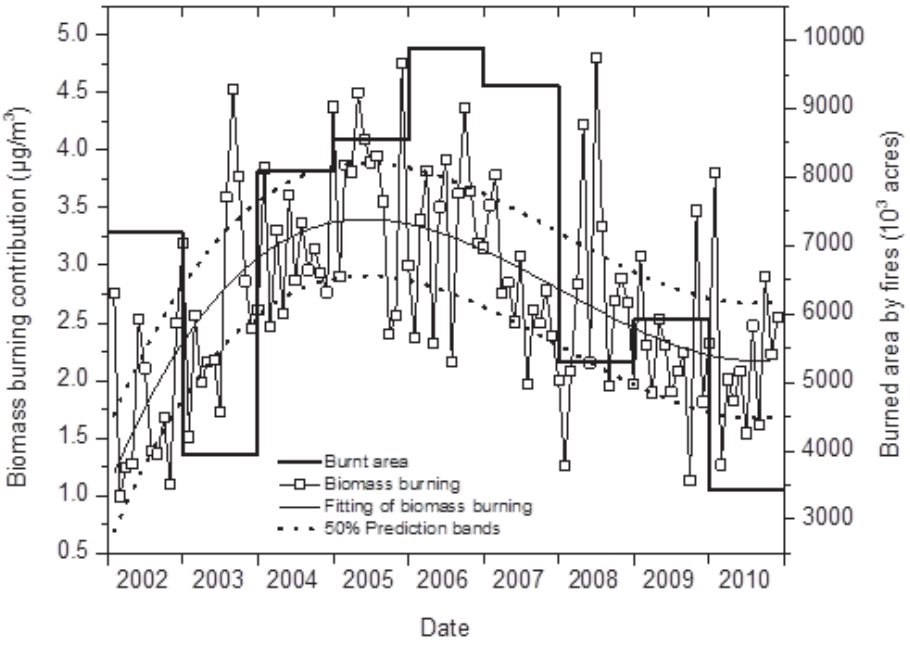

Fig. 5. Annual variation of $PM_{2.5}$ from biomass burning in Little Rock, Arkansas and burnt area by wildfires in the USA for the 2002–2010 period.

ACPD
13, 827–862, 2013

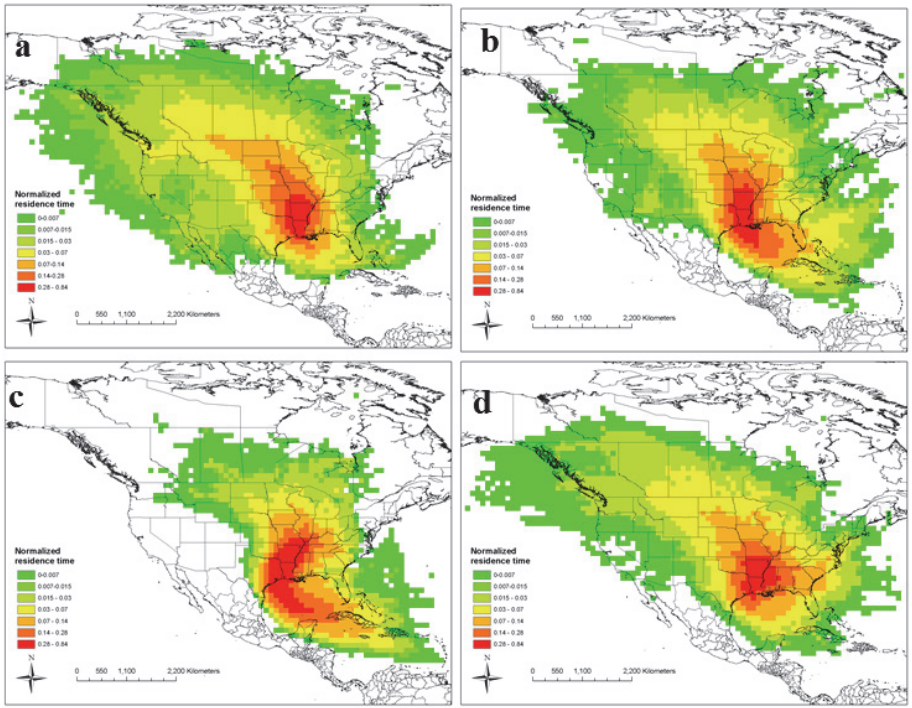

Fig. 6. Percentage of time the air mass parcel is in a horizontal grid cell (0.5° × 0.5°) using backward trajectories at 500 m in winter **(a)**, spring **(b)**, summer **(c)** and fall **(d)**.

ACPD
13, 827–862, 2013

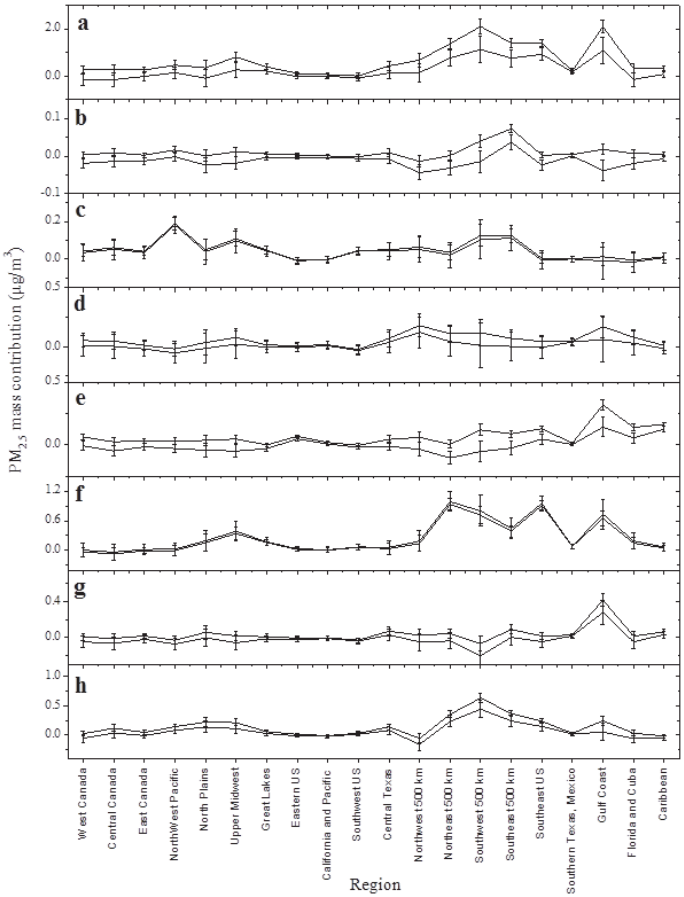

Fig. 7. Contributions of predefined source regions on $PM_{2.5}$ mass **(a)**, primary traffic particles **(b)**, secondary nitrate **(c)**, diesel particles **(d)**, aged sea salt particles **(e)**, secondary sulphate **(f)**, mineral dust particles **(g)** and biomass burning particles **(h)** in Little Rock, Arkansas.

ACPD
13, 827–862, 2013

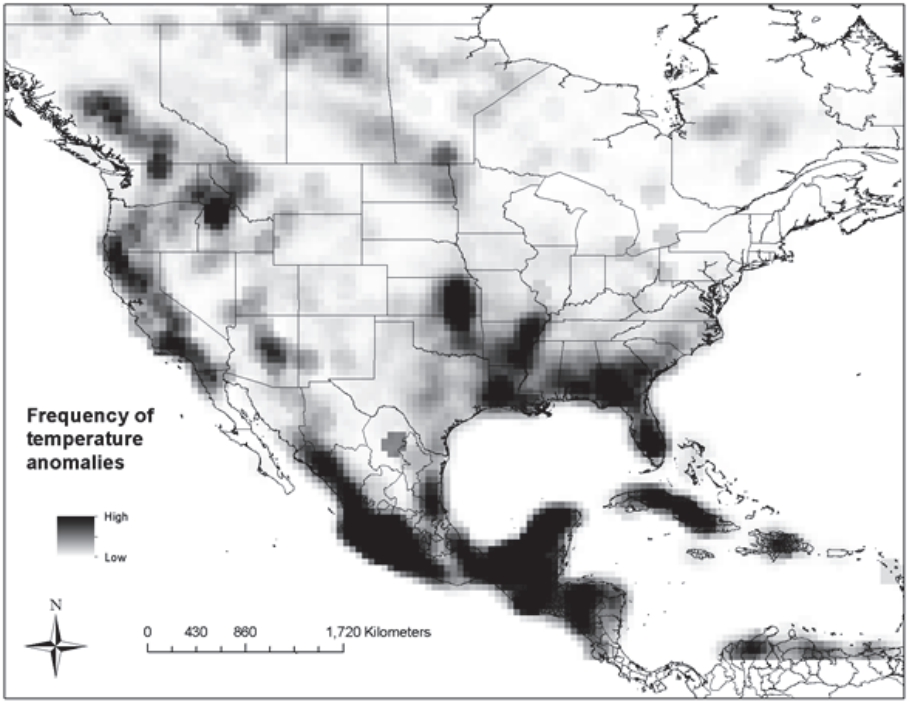

Fig. 8. Cumulative Terra and Aqua MODIS fire and thermal anomalies generated from MODIS data for the monitoring period. The size of the grid cells is 0.5° per side.

ACPD
13, 827–862, 2013